

Preferential Interaction Coefficient for Nucleic Acids and Other Cylindrical Polyions

Emmanuel Trizac*

CNRS, Univ. Paris Sud, UMR8626, LPTMS, Orsay Cedex, F-91405, France, and Center for Theoretical Biological Physics, University of California San Diego, 9500 Gilman Drive MC 0374, La Jolla, California 92093-0374

Gabriel Téllez†

Departamento de Física, Universidad de Los Andes, Apartado Aereo 4976, Bogota, Colombia

Received July 4, 2006; Revised Manuscript Received November 15, 2006

ABSTRACT: The thermodynamics of nucleic acid processes is heavily affected by the electric double layer of microions around the polyions. We focus here on the Coulombic contribution to the salt–polyelectrolyte preferential interaction (Donnan) coefficient, and we report extremely accurate analytical expressions valid in the range of low salt concentration (when polyion radius is smaller than the Debye length). The analysis is performed at the Poisson–Boltzmann level, in cylindrical geometry, with emphasis on highly charged polyions (beyond “counterion condensation”). The results hold for any electrolyte of the form $z_-:z_+$. We also obtain a remarkably accurate expression for the electric potential in the vicinity of the polyion.

Coulombic interactions between salt and polyanions play a key role in the equilibrium and kinetics of nucleic acid processes.¹ A convenient quantity quantifying such interactions and allowing for the analysis and interpretation of their thermodynamics consequences is the so-called preferential interaction coefficient. Several definitions have been proposed and their interrelation studied (see e.g. refs 2–4). In the present work, they are defined as the integrated deficit (with respect to bulk conditions) of co-ions concentration around a rodlike polyion. Our goal is to provide analytical expressions describing the effect of salt concentration and polyion structural parameters on the preferential interaction coefficient, for a broad class of asymmetric electrolytes. For symmetric electrolytes, it will be shown that our formulas improve upon existing analytical results. For other asymmetries, they seem to have no counterpart in the literature. Our analysis holds for highly (i.e., beyond counterion condensation^{5,6}) and uniformly charged cylindrical polyions and is explicitly limited to the low salt regime (i.e., when the polyion radius a is smaller than the Debye length $1/\kappa$). These conditions are most relevant for RNA or DNA in their single-, double-, or triple-strand forms.

As in several previous approaches,^{7–10} we adopt the mean-field framework of Poisson–Boltzmann equation, in a homogeneous dielectric background of permittivity ϵ . The same starting point has proven relevant for related structural physical chemistry studies of nucleic acids.¹¹ In a $z_-:z_+$ electrolyte, the dimensionless electrostatic potential $\phi = e\varphi/kT$ (with $e > 0$ the elementary charge and kT thermal energy) then obeys the equation¹²

$$\frac{1}{r} \frac{d}{dr} \left(r \frac{d\phi}{dr} \right) = \frac{\kappa^2}{z_+ + z_-} [e^{z_- \phi} - e^{-z_+ \phi}] \quad (1)$$

where r is the radial distance to the rod axis. The valencies z_+ and z_- of salt ions are both taken positive. Denoting derivative

with a prime, the boundary conditions read $r\phi'(r) = 2\xi > 0$ at the polyion radius ($r = a$) and $\phi \rightarrow 0$ for $r \rightarrow \infty$. The latter condition expresses the infinite dilution of polyion limit and ensures that the whole system is electrically neutral, since it (indirectly) implies that $r\phi' \rightarrow 0$ for $r \rightarrow \infty$. We consider a negatively charged polyanion for which $\phi < 0$, and the line charge density reads $\lambda = -e\xi/l_B < 0$, where $l_B = e^2/(\epsilon kT)$ denotes the Bjerrum length (0.71 nm in water at room temperature). Finally, the Debye length is defined from the bulk ionic densities n_+^∞ and n_-^∞ through $\kappa^2 = 4\pi l_B(z_+^2 n_+^\infty + z_-^2 n_-^\infty)$.

The Coulombic contribution to the anionic preferential interaction coefficient is defined as^{7–10,13}

$$\Gamma = \kappa^2 \int_a^\infty (e^{z_- \phi} - 1) r dr \quad (2)$$

while its cationic counterpart follows from electroneutrality. This quantity—which provides a measure of the Donnan effect¹⁴—can be expressed in closed form as a function of the electrostatic potential (see Appendix A). As can be seen in (A3) and (A4), Γ depends exponentially on the surface potential ϕ_0 , so that deriving a precise analytical expression is a challenging task. Furthermore, we are interested here in the limit $\kappa a < 1$ (including the regime $\kappa a \ll 1$), which is analytically more difficult than the opposite high salt situation where to leading order the charged rod behaves as an infinite plane, and curvature corrections can be perturbatively included.^{15–17}

We will proceed in two steps. Focusing first on the surface potential $\phi_0 = \phi(a)$, we make use of recent results¹⁸ that have been obtained from a mapping of eq 1 onto a Painlevé type III problem.^{19–21} The exact expressions thereby derived only hold for 1:1, 1:2, and 2:1 electrolytes but may be written in a way that is electrolyte independent. This remarkable feature is specific to the short distance behavior of ϕ and has been overlooked so far, since not only short distance but also large distance properties have been studied.¹⁸ We are then led to conjecture that the corresponding expression holds for *any* binary electrolyte $z_-:z_+$, and we explicitly check the relevance of our assumption on several specific examples.

* Corresponding author. E-mail: trizac@lptms.u-psud.fr.

† E-mail: gtellez@uniandes.edu.co

Table 1. Values of \mathcal{C} Appearing in Eq 4 as a Function of Electrolyte Asymmetries^a

z_+/z_-	1/10	1/3	1/2	1	2	3	10
\mathcal{C}	-2.51	-1.94	-1.763	-1.502	-1.301	-1.21	-1.06

^a For $z_+/z_- = 1, 1/2,$ and $2,$ \mathcal{C} is known analytically from the results of ref 18. The corresponding values are recalled in Appendix B. For other values of z_+/z_- , \mathcal{C} has been determined numerically; see in particular Figure 6 of Appendix B.

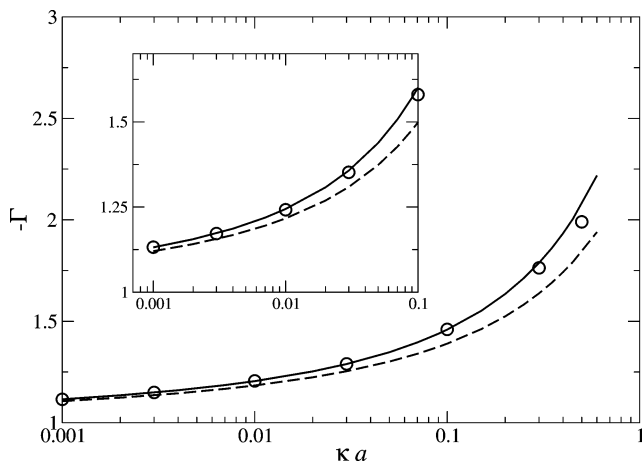


Figure 1. Preferential interaction coefficient for a 1:1 salt. The main graph corresponds to ss-RNA with reduced line charge $\xi = 2.2$ while the inset is for ds-RNA ($\xi = 5$). The circles correspond to the value of (2) following from the numerical solution of eq 1. The prediction of eq 5 with $\tilde{\mu}$ given by (4) and $\mathcal{C} \approx -1.502$, shown with the continuous curve, is compared to that of ref 9, shown with the dashed line. As in all other figures, the opposite of Γ is displayed, to consider a positive quantity.

Technical details are deferred to the appendices. It is in particular concluded in Appendix B that the surface potential may be written

$$e^{-z_+\phi_0} \approx \frac{2(z_+ + z_-)}{z_+(\kappa a)^2} [(z_+\xi - 1)^2 + \tilde{\mu}^2] \quad (3)$$

where

$$\tilde{\mu} \approx \frac{-\pi}{\log(\kappa a) + \mathcal{C} - (z_+\xi - 1)^{-1}} \quad (4)$$

Expression 4 is valid for $\kappa a < 1$ and $z_+\xi > 1$ [in fact, $z_+\xi > 1 + \mathcal{O}(1/|\log \kappa a|)$]. These conditions are easily fulfilled for nucleic acids. The “constant” \mathcal{C} appearing in (3) depends smoothly on the ratio z_+/z_- but is otherwise salt and charge independent. We report in Table 1 its values for several electrolyte asymmetries. The decrease (in absolute value) of \mathcal{C} when z_+/z_- increases is a signature of more efficient (nonlinear) screening with counterions of higher valencies.

From eq 3 and the results of Appendix B, our approximation for Γ takes a simple form

$$\Gamma \approx -\frac{z_-}{z_+}(1 + \tilde{\mu}^2) \quad (5)$$

This expression is tested in Figures 1 and 2 against the “true” numerical results that serve as a benchmark. In Figure 1 which corresponds to a monovalent salt (or more generally a $z:z$ electrolyte), we also show the prediction of ref 9, which is, to our knowledge, the most accurate existing formula for a 1:1 salt. For the technical reasons discussed in Appendix B, and

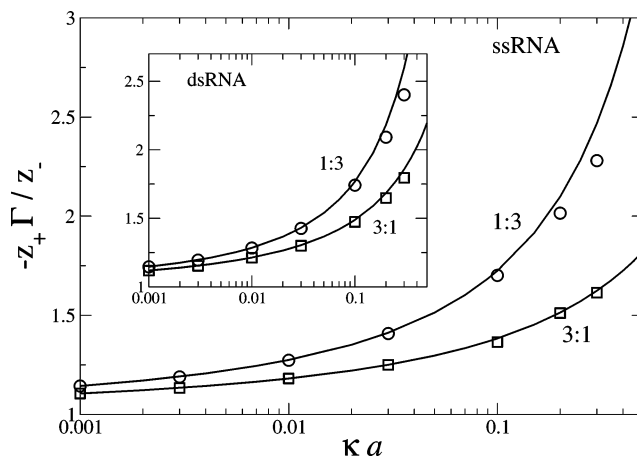


Figure 2. Same as Figure 1 for a 1:3 and a 3:1 electrolyte. From Table 1, we have $\mathcal{C} \approx -1.21$ in the 1:3 case and conversely $\mathcal{C} \approx -1.94$ in the 3:1 case. The symbols correspond to the numerical solution of eq 1, and the continuous curves show the results of eq 5 with again $\tilde{\mu}$ given by eq 4.

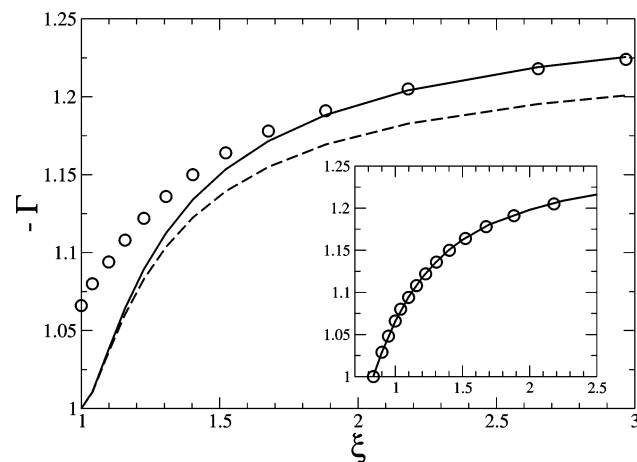


Figure 3. Preferential interaction coefficient for a 1:1 salt (hence $\mathcal{C} \approx -1.502$) and $\kappa a = 10^{-2}$. The circles show the numerical solution of PB theory (1), the continuous curve is for (5) with (4), and the dashed line is the prediction of ref 9. Although approximation (4) breaks down at low ξ , the inset shows that $\tilde{\mu}$ following from the solution of eq C2 gives through (5) a Γ (continuous curve) that is in excellent agreement with the “exact one”, shown with circles as in the main graph.

that are evidenced in Figure 6, our expression improves that of Shkel, Tsoodikov, and Record,⁹ particularly at lower salt content. For 1:2 and 2:1 salts, we expect eq 5 to be also accurate since it is based on exact expansions. The situation of other salt asymmetries is more conjectural (see Appendix B), but eq 5 is nevertheless in remarkable agreement with the full solution of eq 1 (see Figure 2). To be specific, in both Figures 1 and 2, the relative accuracy of our approximation is better than 0.2% for $\kappa a = 10^{-2}$ (for both ss and ds RNA parameters). At $\kappa a = 0.1$, the accuracy is on the order of 1%.

As illustrated in Figure 3, approximation 4 assumes that $z_+\xi > 1$. The corresponding expression for Γ therefore breaks down when ξ is too low. More general expressions, still for $\kappa a < 1$, may be found in Appendix C. The inset of Figure 3 offers an illustration and shows that the limitations of approximation 4 may be circumvented at little cost, providing a quasi-exact value for Γ . Moreover, it is shown in this appendix that for $z_+\xi = 1$ $\tilde{\mu}$ reads

$$\tilde{\mu} \approx \frac{-\pi/2}{\log(\kappa a) + \mathcal{C}} \quad (6)$$

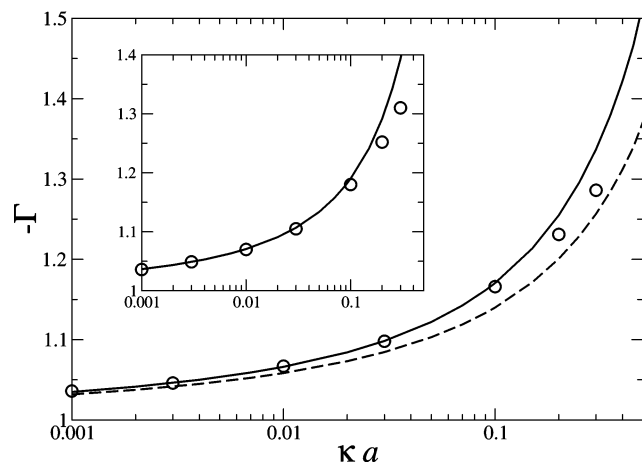


Figure 4. Same as Figure 1 for $\xi = 1$ and $z_+/z_- = 1$. The same quantities are shown: our prediction for Γ [eqs 5 and 6 with $\mathcal{C} \approx -1.502$] is compared to that of ref 9. The inset shows $-z_+\Gamma/z_-$ for a 1:2 salt such as MgCl_2 where \mathcal{C} takes the value -1.301 . Circles: numerical data; curve: our prediction.

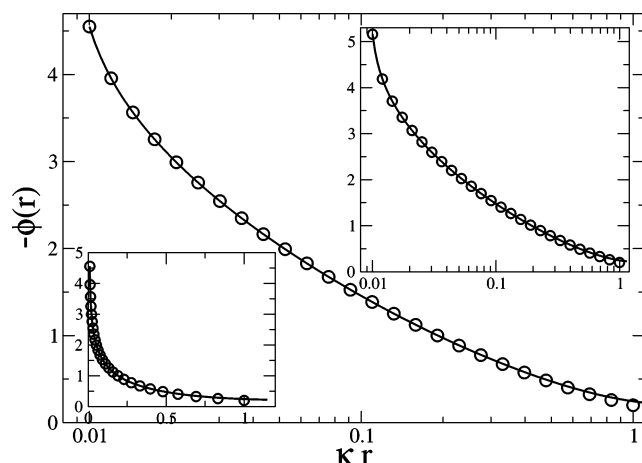


Figure 5. Opposite of the electric potential vs radial distance in a 1:3 electrolyte with $\kappa a = 10^{-2}$. The continuous curve shows the prediction of eq C1 with $\tilde{\mu}$ given by (4); the circles show the numerical solution of eq 1. The potential for $\xi = 2.2$ is shown in the main graph on a log-linear scale and on a linear scale in the lower inset. The upper inset is for $\xi = 5$.

On the other hand, eq 3 still holds. The corresponding Γ is shown in Figure 4.

We provide in Appendix C a general expression of the short scale (i.e., valid up to $\kappa r \sim 1$) radial dependence of the electric potential (see eq C1). The bare charge should not be too low [more precisely, one must have $\xi > \xi_c$ with ξ_c given by eq C5], and $\tilde{\mu}$, which encodes the dependence on ξ , follows from solving eq C2. In general, the corresponding solution should be found numerically. However, one can show (a) that $\tilde{\mu}$ vanishes for $\xi = \xi_c$, (b) that $\tilde{\mu}$ takes the value (6) when $z_+\xi = 1$, and (c) that $\tilde{\mu}$ is given by (4) when $z_+\xi$ exceeds unity by a small and salt-dependent amount. In practice, for DNA and RNA, we have $\xi > 2$, and eq 4 provides excellent results whenever $\kappa a < 0.1$. To illustrate this, we compare in Figure 5 the potential following from the analytical expression C1 to its numerical counterpart. We do not display 1:1, 1:2, and 2:1 results since in these cases eq C1 is obtained from an exact expansion and fully captures the r dependence of the potential. For the asymmetry 1:3, Figure 5 shows that the relatively simple form (C1) is very reliable. A similar agreement has been found for all couples $z_-:z_+$ sampled, with the trend that the validity of (C1) extends to larger distances as z_+/z_- is decreased. In

this respect, the agreement shown in Figure 5 for which z_+/z_- is quite high (3) is one of the “worst” observed.

Conclusion

The polyion ion preferential interaction coefficient Γ describes the exclusion of co-ions in the vicinity of a polyelectrolyte in an aqueous solution. We have obtained an accurate expression for Γ in the regime of low salt ($\kappa a < 1$). The present results are particularly relevant for highly charged polyions ($z_+\xi > 1$, that is, beyond the classical Manning threshold²²) but are somewhat more general and hold in the range $\xi_c < \xi < 1$, where ξ stands for the line charge per Bjerrum length and ξ_c is a salt-dependent threshold, given by eq C5. Our formulas have been shown to hold for arbitrary mixed salts of the form $z_-:z_+$ (magnesium chloride, cobalt hexamine, etc.). They have been derived from exact expansions valid in 1:1,1:2, and 2:1 cases, from which a more general conjecture has been inferred. The validity of this conjecture, backed up by analytical arguments, has been extensively tested for various values of z_+/z_- , polyion charge, and salt content. These tests have provided the numerical value of the constant \mathcal{C} reported in Table 1, which only depends on the ratio z_+/z_- . As a byproduct of our analysis, we have obtained a very accurate expression for the electric potential in the vicinity of the charged rod ($r < \kappa^{-1}$).

It should be emphasized that the validity of our mean-field description relying on the nonlinear Poisson–Boltzmann equation depends on the valency of counterions (z_+) and to a lesser extent on the value of z_- .^{12,23} For the 1:1 case in a solvent like water at room temperature, microionic correlations can be neglected up to a salt concentration of 0.1 M.⁸ For $z_+ \geq 2$ or in solvents of lower dielectric permittivity, they play a more important role. Our results however provide mean-field benchmarks from analytical expressions, from which the effects of correlations may be assessed in cases where they cannot be ignored (see e.g. ref 8 for a detailed discussion).

Acknowledgment. This work was supported by a ECOS Nord/COLCIENCIAS action of French and Colombian cooperation. G.T. acknowledges partial financial support from Comité de Investigaciones, Facultad de Ciencias, Universidad de los Andes. This work has been supported in part by the NSF PFC-sponsored Center for Theoretical Biological Physics (Grants PHY-0216576 and PHY-0225630).

Appendix A

In order to explicitly relate the preferential coefficient Γ in (2) to the electric potential, we follow a procedure similar to that which leads to an analytical solution in the cell model, without added salt.²⁴ Implicit use will be made of the boundary conditions associated with (1). First, integrating eq 1, one gets

$$[r'\phi'(r')]_a^r = \frac{\kappa^2}{z_+ + z_-} \int_a^r (e^{-z_+\phi} - e^{-z_-\phi}) r' dr' \quad (\text{A1})$$

where the notation $[F(r')]_a^r = F(r) - F(a)$ has been introduced. Then, multiplying eq 1 by $r^2\phi'$ and integrating, we obtain

$$\frac{z_+ + z_-}{2\kappa^2} [(r'\phi')^2]_a^r = - \left[r'^2 \frac{e^{-z_+\phi}}{z_+} + r'^2 \frac{e^{-z_-\phi}}{z_-} \right]_a^r + \int_a^r 2r' \left(\frac{e^{-z_+\phi}}{z_+} + \frac{e^{-z_-\phi}}{z_-} \right) dr' \quad (\text{A2})$$

Combining both relations with adequate weights, in order to suppress the integral over counterion (+) density, we have

$$\int_a^\infty r' (e^{z-\phi} - 1) dr' = \frac{z_+ z_-}{\kappa^2} \left(\xi^2 - \frac{2\xi}{z_+} \right) - \frac{a^2}{2(z_+ + z_-)} \{ z_+ (e^{z_-\phi_0} - 1) + z_- (e^{-z_+\phi_0} - 1) \} \quad (\text{A3})$$

where $\phi_0 = \phi(a)$ is the surface potential. Equation A3 will turn useful in the formulation of a general conjecture concerning the surface potential ϕ_0 (see Appendix B). We also note that for the systems under investigation here the surface potential is quite high, and a very good approximation to (A3) is

$$\int_a^\infty r' (e^{z-\phi} - 1) dr' \approx \frac{z_+ z_-}{\kappa^2} \left(\xi^2 - \frac{2\xi}{z_+} \right) - \frac{a^2 z_- e^{-z_+\phi_0}}{2(z_+ + z_-)} \quad (\text{A4})$$

Appendix B

We start by analyzing a 1:1 electrolyte, for which it has been shown^{19,20} that the short distance behavior reads

$$e^{\phi/2} = \frac{\kappa r}{4\mu} \sin \left[2\mu \log \left(\frac{\kappa r}{8} \right) - 2\Psi(\mu) \right] + O(\kappa r)^4 \quad (\text{B1})$$

where Ψ denotes the argument of the Euler Gamma function $\Psi(x) = \arg[\Gamma(ix)]$.^{19,20} In (B1), μ denotes the smallest positive root of

$$\tan[2\mu \log(\kappa a/8) - 2\Psi(\mu)] = \frac{2\mu}{\xi - 1} \quad (\text{B2})$$

Expressions B1 and B2 require that ξ exceeds a salt-dependent threshold [denoted ξ_c below and given by eq C5] that is always smaller than 1.¹⁸ They thus always hold for $\xi \geq 1$ and in particular encompass the interesting limiting case $\xi = 1$, which is sufficient for our purposes. For large ξ , we have proposed in ref 18 an approximation which amounts to linearizing the argument of the tangent in (B1) in the vicinity of $-\pi$ and similarly linearizing Ψ to first order: $\Psi(x) \approx -\pi/2 - \gamma x + \mathcal{O}(x^3)$, where γ is the Euler constant, close to 0.577. It turns out, however, that finding accurate expressions for $\exp(-z_+\phi_0)$, which is useful for the computation of the preferential interaction coefficient, requires to include the first nonlinear correction in the expansion of the tangent. After some algebra, we find

$$\mu \approx \frac{-\pi/2}{\log(\kappa a) + \mathcal{C} - (\xi - 1)^{-1}} + \frac{\pi^3}{6(\log(\kappa a) + \mathcal{C} - (\xi - 1)^{-1})^4} \left[\frac{1}{(\xi - 1)^3} + \frac{\psi^{(2)}(1)}{8} \right] \quad (\text{B3})$$

where the constant $\mathcal{C} = \mathcal{C}^{1:1}$ reads $\mathcal{C}^{1:1} = \gamma - \log 8 \approx -1.502$ and $\psi^{(2)}(1) = d^3 \ln \Gamma(x)/dx^3|_{x=1}$. From (B3) and (B3) where the sinus is expanded to third order, we obtain

$$(\kappa a)^2 e^{-\phi_0} \approx 4[(\xi - 1)^2 + \tilde{\mu}^2] \quad (\text{B4})$$

where $\tilde{\mu}$ is given by

$$\tilde{\mu} \approx \frac{-\pi}{\log(\kappa a) + \mathcal{C} - (z_+\xi - 1)^{-1}} \quad (\text{B5})$$

In writing (B5), we have introduced the change of variable $\tilde{\mu} = 2\mu$.²⁵ The reason is that similar changes for other electrolyte asymmetries allows to put the final result in a ‘‘universal’’ (electrolyte independent) form (see below). A similar reason holds for introducing z_+ , here equal to 1, in the denominator of (B5).

The functional proximity between our expressions and those reported in ref 9 in the very same context is striking. We note, however, that our $\tilde{\mu}$ (denoted β in ref 9) involves a different constant \mathcal{C} . More importantly, the functional form of (B1) differs from that given in ref 9. The comparison of the performances of our results with those of ref 9 is addressed below and is also discussed in the main text.

Performing a similar analysis as above in the 1:2 case where $z_+ = 2$ and $z_- = 1$, we obtain from the expressions derived in ref 18:

$$(\kappa a)^2 e^{-z_+\phi_0} \approx 3[(\xi - 1)^2 + \tilde{\mu}^2] \quad (\text{B6})$$

and similarly in the 2:1 case ($z_+ = 1$, $z_- = 2$)

$$(\kappa a)^2 e^{-z_+\phi_0} \approx 6[(\xi - 1)^2 + \tilde{\mu}^2] \quad (\text{B7})$$

In both cases, provided again that ξ is not too low (see below), $\tilde{\mu}$ is given by (B5),²⁶ with however a different numerical value for \mathcal{C} [$\mathcal{C}^{1:2} = \gamma - (3 \log 3)/2 - (\log 2)/3 \approx -1.301$ and $\mathcal{C}^{2:1} = \gamma - (3 \log 3)/2 - \log 2 \approx -1.763$].

The similarity of expressions B4, B6, and B7 leads to conjecture that this form holds for any $z_-:z_+$ electrolyte:

$$(\kappa a)^2 e^{-z_+\phi_0} \approx \mathcal{L}[(z_+\xi - 1)^2 + \tilde{\mu}^2] \quad (\text{B8})$$

We then have to determine the prefactor \mathcal{L} as a function of z_+ and z_- . To this end, we make use of the exact relation (A3) [or equivalently (A4)], where in the limit of large ξ the left-hand side is finite while the two terms on the right-hand side diverge. This yields the leading order behavior:

$$(\kappa a)^2 \exp(-z_+\phi_0) \sim 2 \frac{z_+ + z_-}{z_+} (z_+\xi - 1)^2 \quad (\text{B9})$$

It then follows that $\mathcal{L} = 2(z_+ + z_-)/z_+$ so that our general expression B8 takes the form

$$(\kappa a)^2 e^{-z_+\phi_0} \approx 2 \frac{z_+ + z_-}{z_+} [(z_+\xi - 1)^2 + \tilde{\mu}^2] \quad (\text{B10})$$

This expression holds regardless of the approximation used for $\tilde{\mu}$. If eq B5 is used, then $z_+\xi$ should not be too close to unity (see Appendix C for more general results including the case $z_+\xi = 1$).

In order to test the accuracy of (B10) in conjunction with (B5), we have solved numerically eq 1 for several values of $\kappa a < 1$ and electrolyte asymmetry and checked that for several different values of $z_+\xi > 1$ the quantity

$$\mathcal{Q} = -\pi \left[(\kappa a)^2 e^{-z_+\phi_0} \frac{z_+}{2(z_+ + z_-)} - (z_+\xi - 1)^2 \right]^{-1/2} - \log(\kappa a) + (z_+\xi - 1)^{-1} \quad (\text{B11})$$

is a constant \mathcal{C} , which only depends on z_+/z_- but not on salt and ξ . [It should be borne in mind that eq B5 is a small κa and large ξ expansion, which becomes increasingly incorrect as κa is increased and/or ξ lowered.] This is quite a stringent test (since the two terms on the right-hand side of (B11) are large and close) which requires high numerical accuracy. This is achieved following the procedure outlined in ref 27. In doing so, we confirm the validity of (B10) and collect the values of \mathcal{C} given in Table 1. In the 1:1 case, we predict that $\mathcal{C} = \gamma - \log 8 \approx -1.507$, in excellent agreement with the numerical data of Figure 6. On the other hand, the prediction of ref 9 that \mathcal{Q}

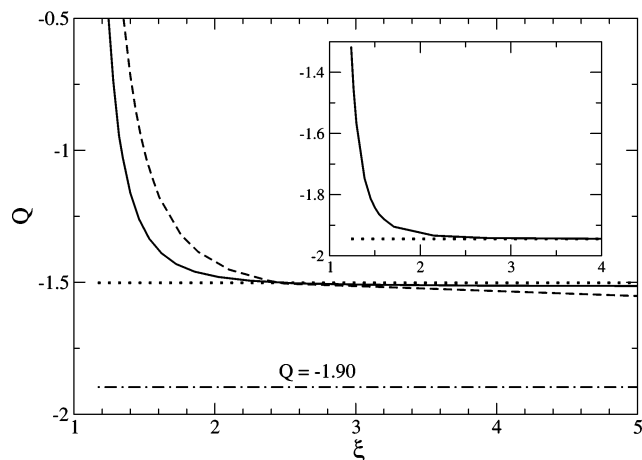


Figure 6. Plot of the quantity \mathcal{Q} defined in (B11) vs line charge ξ for a 1:1 electrolyte at $\kappa a = 10^{-3}$ (continuous curve) and $\kappa a = 10^{-1}$ (dashed curve). The value reached at large ξ is compared to the prediction of⁹ $\mathcal{Q} \rightarrow e^\gamma + \log 2 - \gamma \approx -1.90$ (horizontal dashed-dotted line) whereas eqs B10 and B5 imply $\mathcal{Q} \rightarrow \gamma - \log 8 \approx -1.50$, shown by the horizontal dotted line. The inset shows the same quantity for a 3:1 electrolyte at $\kappa a = 10^{-5}$. [Such a very low value is required to determine precisely the value of the asymptotic constant \mathcal{C} , which can subsequently be used at experimentally relevant (higher) salt concentrations.] Here, we obtain $\mathcal{Q} \rightarrow -1.94$ (dotted line), which is the value reported for \mathcal{C} in Table 1.

reaches a constant close to -1.90 (shown by the horizontal dashed line in Figure 6) is incorrect. Figure 6 shows that the quality of expression B10 deteriorates when κa increases, as expected. It is noteworthy, however, that for $\kappa a = 10^{-1}$ its accuracy is excellent whenever $\xi > 2$. The inset of Figure 6 shows the validity of (B10) for a 3:1 electrolyte. When $z_+\xi$ is close to 1, eq B5 becomes an irrelevant approximation to the solution of eq B2 and can therefore not be inserted into the general formula B10. This explains the large deviations between \mathcal{Q} and the asymptotic value \mathcal{C} observed in Figure 6 for the lower values of ξ reported. We come back to this point in Appendix C.

The present results hold for $z_+\xi > 1 + \mathcal{O}(1/|\log \kappa a|)$. In this regime, our analysis shows that eq B10 [with $\tilde{\mu}$ given by (B5)] is correct up to order $1/\log^4(\kappa a)$ for any (z_-, z_+) . On the other hand, the results of ref 9, valid in the 1:1 case, appear to be correct to order $1/\log^2(\kappa a)$. In addition, our expression for the surface potential may be generalized to a broader range of ξ values, and an expression for the short distance dependence of the electric potential may also be provided. This is the purpose of Appendix C.

Appendix C

In Appendix B, the “universal” results valid for all (z_+, z_-) have been unveiled partly by a change of variable $\mu \rightarrow \tilde{\mu}$ from existing expressions.¹⁸ In light of these results and of their accuracy (assessed in particular by the precision reached for the preferential interaction coefficient), it is tempting to go further without invoking approximations of (B2) or related expressions for other asymmetries than 1:1. Inspection of the results given in ref 18 for the 1:1, 1:2, and 2:1 cases lead, with again the help of (A4), to the conjecture that

$$e^{z_+\phi/2} \approx \frac{-\kappa r}{\tilde{\mu}} \sqrt{\frac{z_+}{2(z_+ + z_-)}} \sin[\tilde{\mu} \log(\kappa r) + \tilde{\mu} \mathcal{C}] \quad (\text{C1})$$

with

$$\tan[\tilde{\mu} \log(\kappa a) + \tilde{\mu} \mathcal{C}] = \frac{\tilde{\mu}}{z_+\xi - 1} \quad (\text{C2})$$

We emphasize that (C1), much as (B1), is a short distance expansion and typically holds for $\kappa r < 1$ (hence the requirement that $\kappa a < 1$). In Appendix D we give further analytical support for conjecture (C1). A typical plot showing the accuracy of (C1) is provided in the main text (Figure 5). For $\kappa r < 0.1$, the agreement with the exact result is better than 0.1% and becomes progressively worse at higher distances (20% disagreement at $\kappa r = 1$).

From (C1), it follows that the integrated charge $q(r)$ in a cylinder of radius r [that is $q(r) = -r\phi'(r)/2$] reads

$$z_+q(r) = -1 + \tilde{\mu} \tan\left[\tilde{\mu} \log\left(\frac{r}{R_M}\right)\right] \quad (\text{C3})$$

where the so-called Manning radius^{18,28,29} is given by

$$\kappa R_M = \exp\left(-\mathcal{C} - \frac{\pi}{2\tilde{\mu}}\right) \quad (\text{C4})$$

The Manning radius is a convenient measure of the counterion condensate thickness. It is the point r where not only $z_+q(r) = 1$ but also where $q(r)$ vs $\log r$ exhibits an inflection point.³⁰ For high enough ξ , the logarithmic dependence of $1/\tilde{\mu}$ with salt [see (B5)] is such that $R_M \propto \kappa^{-1/2}$.

The two relations C1 and C2 encompass those given in Appendix B and allow to investigate the regime $z_+\xi_c < z_+\xi$ and in particular the case $z_+\xi = 1$, the so-called Manning threshold.⁵ However, (C1) and (C2) are not valid for $\xi < \xi_c$, with

$$z_+\xi_c = 1 + \frac{1}{\log \kappa a + \mathcal{C}} \quad (\text{C5})$$

Note that $\xi_c < 1$, since the constant \mathcal{C} is negative and that salt should fulfill $\kappa a < 1$. For $\kappa a = 10^{-2}$ and $z_+/z_- = 1$, we obtain $\xi_c \approx 0.836$. This is precisely the point where $-\Gamma = 1$ in the inset of Figure 3. This inset also shows that the value of Γ resulting from the use of the solution of (C2) is remarkably accurate.

At this point, it seems useful to investigate the Manning threshold case $z_+\xi = 1$ (which corresponds to the onset of counterion condensation when $\kappa a \rightarrow 0$ ^{5,18,30}). It is readily seen that the solution of (C2) reads

$$\tilde{\mu}^{z_+\xi=1} = \frac{-\pi/2}{\log(\kappa a) + \mathcal{C}} \quad (\text{C6})$$

which should be inserted in (C1) to obtain the potential profile or in (5) to get the interaction coefficient.

Appendix D

In this appendix we give further support for the conjecture (C1) which gives the short distance expansion of the electric potential. Let us suppose initially that the charge is below the Manning threshold $\xi < \xi_c$. It is straightforward to verify that Poisson–Boltzmann eq 1 admits solutions which behave as $\phi(r) = -2A \ln(\kappa r) + \ln B + \mathcal{O}(1)$ for $\kappa r \ll 1$. Injecting this expansion into eq 1 allows us to compute higher order terms. To study the regime beyond the Manning threshold, we compute all higher order terms of the form $r^{2n(1+z_+A)}$ (for a negatively charged macroion) and $r^{2n(1-z_+A)}$ (for a positively charged macroion), with n a positive integer. These terms turn out to present themselves as the series expansion of the logarithm;

thus, resumming them we obtain

$$\phi(r) = -2A \ln(\kappa r) + \ln B + \frac{2}{z_+} \ln \left[1 - \frac{z_+ B^{-z_+} (\kappa r)^{2(1+z_+A)}}{8(z_+ + z_-)(1 + z_+A)^2} \right] - \frac{2}{z_-} \ln \left[1 - \frac{z_- B^{-z_-} (\kappa r)^{2(1-z_-A)}}{8(z_+ + z_-)(1 - z_-A)^2} \right] + \dots \quad (\text{D1})$$

The dots represent terms of order $r^{2n(1+z_+A)+2m(1-z_-A)}$ with n and m two nonzero positive integers. When the Manning threshold is approached, $z_+A + 1 = 0$ for negatively charged macroion, the terms $r^{2n(1+z_+A)}$ (second line of eq D1) become of order one, but the rest of the terms (third line of eq D1 and dots) remain higher order: a change in the small distance behavior of ϕ occurs. A similar situation is reached for $1 - z_-A = 0$, which is the Manning threshold for a positively charged macroion.

A and B in the previous equations are constants of integration, which should be determined with the boundary conditions $r\phi'(r) = 2\xi$ at the polyion radius ($r = a$) and $\phi \rightarrow 0$ for $r \rightarrow \infty$. Thus, to proceed further, we have to connect the long and the short distance behavior of ϕ . This connection problem has been only solved in the cases 1:1, 1:2, and 2:1 in refs 19 and 31. In particular, once A has been chosen (notice that for $a = 0$, $A = -\xi$), B should be one and only one function of A in order to satisfy $\phi \rightarrow 0$ for $r \rightarrow \infty$. The results from refs 19 and 31 show that

$$B = 2^{6A} \gamma((1+A)/2)^2 \quad (1:1)$$

$$B = 3^{3A} 2^{2A} \gamma(2(1+A)/3) \gamma((1+A)/3) \quad (1:2)$$

$$B = 3^{3A} 2^{2A} \gamma((1+2A)/3) \gamma((2+A)/3) \quad (2:1) \quad (\text{D2})$$

where $\gamma(x) = \Gamma(x)/\Gamma(1-x)$. B turns out to have some interesting properties in the cases 1:1, 1:2, and 2:1, where its exact expression D2 is known. Namely, at the Manning threshold $1 + z_+A = 0$

$$\lim_{A \rightarrow -1/z_+} \frac{z_+ B^{-z_+}}{8(z_+ + z_-)(1 + z_+A)^2} = 1 \quad (\text{D3})$$

Furthermore, if we put $1 + z_+A = i\tilde{\mu}$ and define

$$e^{2i\Psi(\tilde{\mu})} = \frac{z_+ B^{-z_+}}{8(z_+ + z_-)(1 + z_+A)^2} \quad (\text{D4})$$

then for $\tilde{\mu} \in \mathbb{R}$, $\Psi(\tilde{\mu}) \in \mathbb{R}$ is a real function of $\tilde{\mu}$, with $\Psi(0) = 0$.

Let us now study the regime beyond the Manning threshold for a negatively charged macroion. From eq D1 we can write

$$e^{z_+\phi(r)/2} \sim (\kappa r)^{-z_+A} B^{z_+/2} \left(1 - \frac{z_+ B^{-z_+} (\kappa r)^{2(1+z_+A)}}{8(z_+ + z_-)(1 + z_+A)^2} \right) \quad (\text{D5})$$

neglecting terms of higher order when z_+A is close to -1 .

Let us conjecture that the properties of B as a function of A presented above hold in the general case $z_-:z_+$. Then using the parameter $\tilde{\mu}$ defined above we find after some simple algebra

$$e^{z_+\phi(r)/2} = \frac{-\kappa r}{\tilde{\mu}} \sqrt{\frac{z_+}{2(z_+ + z_-)}} \sin[\tilde{\mu} \log(\kappa r) + \Psi(\tilde{\mu})] + O(r^{3+2z_-z_+}) \quad (\text{D6})$$

Recalling that $|\tilde{\mu}| \ll 1$, we can approximate $\Psi(\tilde{\mu}) \approx \tilde{\mu} \mathcal{C}$, where $\mathcal{C} = \Psi'(0)$. Replacing this approximation into (D6) and imposing the boundary condition $a\phi'(a) = 2\xi$ leads to (C1) and (C2). Numerical values obtained for the constants \mathcal{C} are reported in Table 1, for different charge asymmetries $z_-:z_+$. The previous analysis shows that analytical predictions for \mathcal{C} could be made if the connection problem is solved and the equivalent of expressions D2 are found for the general case $z_-:z_+$.

References and Notes

- (1) Anderson, C. F.; Record, M. T., Jr. *Annu. Rev. Phys. Chem.* **1984**, *33*, 191.
- (2) Eisenberg, H. *Biological Macromolecules and Polyelectrolytes in Solution*; Clarendon: Oxford, 1976.
- (3) Schellman, J. A. *Biophys. Chem.* **1990**, *37*, 121.
- (4) Timasheff, S. M. *Biochemistry* **1992**, *31*, 9857.
- (5) Manning, G. S. *J. Chem. Phys.* **1969**, *51*, 924.
- (6) Oosawa, F. *Polyelectrolytes*; Dekker: New York, 1971.
- (7) Sharp, K. A. *Biopolymers* **1995**, *36*, 227.
- (8) Ni, H.; Anderson, C. F.; Record, M. T., Jr. *J. Phys. Chem. B* **1999**, *103*, 3489.
- (9) Shkel, I. A.; Tsodikov, O. V.; Record, M. T., Jr. *Proc. Natl. Acad. Sci. U.S.A.* **2002**, *99*, 2597.
- (10) Taubes, C. H.; Mohanty, U.; Chu, S. *J. Phys. Chem. B* **2005**, *109*, 21267.
- (11) Gueron, M.; Demaret, J.-Ph.; Filoche, M. *Biophys. J.* **2000**, *78*, 1070.
- (12) Levin, Y. *Rep. Prog. Phys.* **2002**, *65*, 1577.
- (13) In the 1:1 case, our definition differs from the more standard one as found e.g. in ref 9 by a factor 4ξ . The reason for doing so is that this allows easier comparison of the salt dependence of Γ for different values of the polyion charge.
- (14) Donnan, F. G. *Chem. Rev.* **1924**, *1*, 73.
- (15) Shkel, I. A.; Tsodikov, O. V.; Record, M. T., Jr. *J. Phys. Chem. B* **2000**, *104*, 5161.
- (16) Aubouy, M.; Trizac, E.; Bocquet, L. *J. Phys. A: Math. Gen.* **2003**, *36*, 5835.
- (17) Tellez, G.; Trizac, E. *Phys. Rev. E* **2004**, *70*, 011404.
- (18) Trizac, E.; Téllez, G. *Phys. Rev. Lett.* **2006**, *96*, 038302. Téllez, G.; Trizac, E. *J. Stat. Mech.* **2006**, P06018.
- (19) McCoy, B. M.; Tracy, C. A.; Wu, T. T. *J. Math. Phys.* **1977**, *18*, 1058.
- (20) McCaskill, J. S.; Fackerell, E. D. *J. Chem. Soc., Faraday Trans. 2* **1988**, *84*, 161.
- (21) Tracy, C. A.; Widom, H. *Physica A* **1997**, *244*, 402.
- (22) We emphasize that accurate results for Γ , ϕ , etc., may be obtained for $\xi < \xi_c$ from the results given in ref 18. We did not investigate this regime here, since it is of little relevance for nucleic acids.
- (23) Grosberg, A. Y.; Nguyen, T. T.; Shklovskii, B. I. *Rev. Mod. Phys.* **2002**, *74*, 329.
- (24) Fuoss, R. M.; Katchalsky, A.; Lifson, S. F. *Proc. Natl. Acad. Sci. U.S.A.* **1951**, *37*, 579.
- (25) It then appears that the expression given for $\tilde{\mu} = 2\mu$ in (B5) corresponds to the dominant term only in (B3) (the first one on the right-hand side).
- (26) Compared to the expressions given in ref 18 where a parameter μ plays a key role, the corresponding change of variables should be performed: $\tilde{\mu} = 3\mu$ (1:2 case) and $\tilde{\mu} = 3\mu/2$ for 2:1 electrolytes.
- (27) Trizac, E.; Bocquet, L.; Aubouy, M.; von Grünberg, H. H. *Langmuir* **2003**, *19*, 4027.
- (28) Gueron, M.; Weisbuch, G. *Biopolymers* **1980**, *19*, 353.
- (29) O'Shaughnessy, B.; Yang, Q. *Phys. Rev. Lett.* **2005**, *94*, 048302.
- (30) Deserno, M.; Holm, C.; May, S. *Macromolecules* **2000**, *33*, 199.
- (31) Tracy, C. A.; Widom, H. *Commun. Math. Phys.* **1998**, *190*, 697.